Biosensors and Bioelectronics 190 (2021) 113450

Contents lists available at ScienceDirect

Biosensors and Bioelectronics

journal homepage: www.elsevier.com/locate/bios

Nano-immunosorbent assay based on Cas12a/crRNA for ultra-sensitive protein detection

Qiao Zhao [a], Yongchun Pan [b], Xiaowei Luan [b], Yanfeng Gao [b], Xiaozhi Zhao [c], Yinghui Liu [d], Yuzhen Wang [a,**], Yujun Song [b,*]

[a] Key Laboratory of Flexible Electronics & Institute of Advanced Materials, Jiangsu National Synergistic Innovation Center for Advanced Materials, Nanjing Tech University, Nanjing, 211816, China
[b] College of Engineering and Applied Sciences, State Key Laboratory of Analytical Chemistry for Life Science, Nanjing University, Nanjing, 210023, China
[c] Department of Medical Laboratory, Nanjing Drum Tower Hospital Affiliated to Medical College, Nanjing University, Nanjing, 210008, China
[d] College of Life Sciences, Nanjing Normal University, Nanjing, 210023, China

ARTICLE INFO

Keywords:
CRISPR/Cas12a
Gold nanoparticles
Biosensors
Fluorescence
Signal conversion strategy

ABSTRACT

Apart from the great potential in genome editing, the clustered regularly interspaced short palindromic repeat (CRISPR)/Cas system has recently been widely used in biosensing. However, due to the complex and inefficient signal conversion strategies, most of the works focused on nucleic acid analysis rather than protein biomarkers. Herein, by employing DNA-AuNPs (gold nanoparticles) nanotechnology to activate *trans*-cleavage activity of CRISPR/Cas12a, a universal signal transduction strategy was established between *trans*-cleavage of CRISPR/Cas12a and protein analytes. As a result, a sensitive platform was developed for sensing carcinoembryonic antigen (CEA) and prostate specific-antigen (PSA) biomarkers, which was designated as Nano-CLISA (Nano-immunosorbent assay based on Cas12a/crRNA). Nano-CLISA was directly employed to test PSA in clinical samples, indicating its great potential in practical detection. This platform has been used to quantitatively analyze protein at attomolar levels, which was 1000-fold more sensitive than traditional ELISA, and the detection range is 15 times wider than that of traditional ELISA.

1. Introduction

The clustered regularly interspaced short palindromic repeats (CRISPR)-associated proteins (CRISPR/Cas) system has been predominantly deployed in genome editing (Bikard and Barrangou, 2017; Jinek et al., 2012; Pan et al., 2019; Strecker et al., 2019) and molecular diagnosis (Ackerman et al., 2020; Gootenberg et al. 2017, 2018; van Dongen et al., 2020). CRISPR/Cas12a (Cpf1) is a class 2 CRISPR/Cas system, which is composed of single CRISPR RNA (crRNA)-guided endonucleases that bind and cleave DNA (Zetsche et al., 2015). With recent discovery of the indiscriminate collateral cleavage activities (*trans*-cleavage) on single-stranded DNA (ssDNA) (Chen et al., 2018; Li et al., 2018), CRISPR systems demonstrated tremendous potential in nucleic acid analysis. In order to improve the sensitivity, several amplification methods were introduced into CRISPR/Cas12a detection systems, such as polymerase chain reaction (PCR) (Li et al., 2021), recombinase polymerase amplification (RPA) (Yin et al., 2020), loop-mediated isothermal amplification (LAMP) (Qian et al., 2019), etc. For example, a DNA endonuclease-targeted CRISPR trans reporter (DETECTR) method based on Cas12a *trans*-cleavage activation combined with isothermal amplification has been reported to achieve high sensitivity and accuracy for detection of human papillomavirus (HPV) DNA in clinical samples (Chen et al., 2018). However, these amplification strategies are expensive, complex and easy to bring the risk of false positives caused by contamination (Bao et al., 2020; Lin et al., 2021; Nam et al., 2003). Besides, the universality of biosensing platforms based on CRISPR/Cas was limited because of insufficient strategies to transduce the non-nucleic acid analyte recognition event into the *trans*-cleavage activity of CRISPR/Cas. Despite the recent progress that has been made in the detection of non-nucleic acid analysis (Broughton et al., 2020; He et al., 2020; Li et al., 2020; Liang et al., 2019; Xiong et al., 2020; Zhao et al., 2020), there are scarce works devoted to the detection of protein analytes. Therefore, more strategies need to be designed to broaden the biosensing applications of CRISPR/Cas12a

** Corresponding author.
* Corresponding author.
E-mail addresses: iamyzwang@njtech.edu.cn (Y. Wang), ysong@nju.edu.cn (Y. Song).

https://doi.org/10.1016/j.bios.2021.113450
Received 21 May 2021; Received in revised form 16 June 2021; Accepted 17 June 2021
Available online 26 June 2021

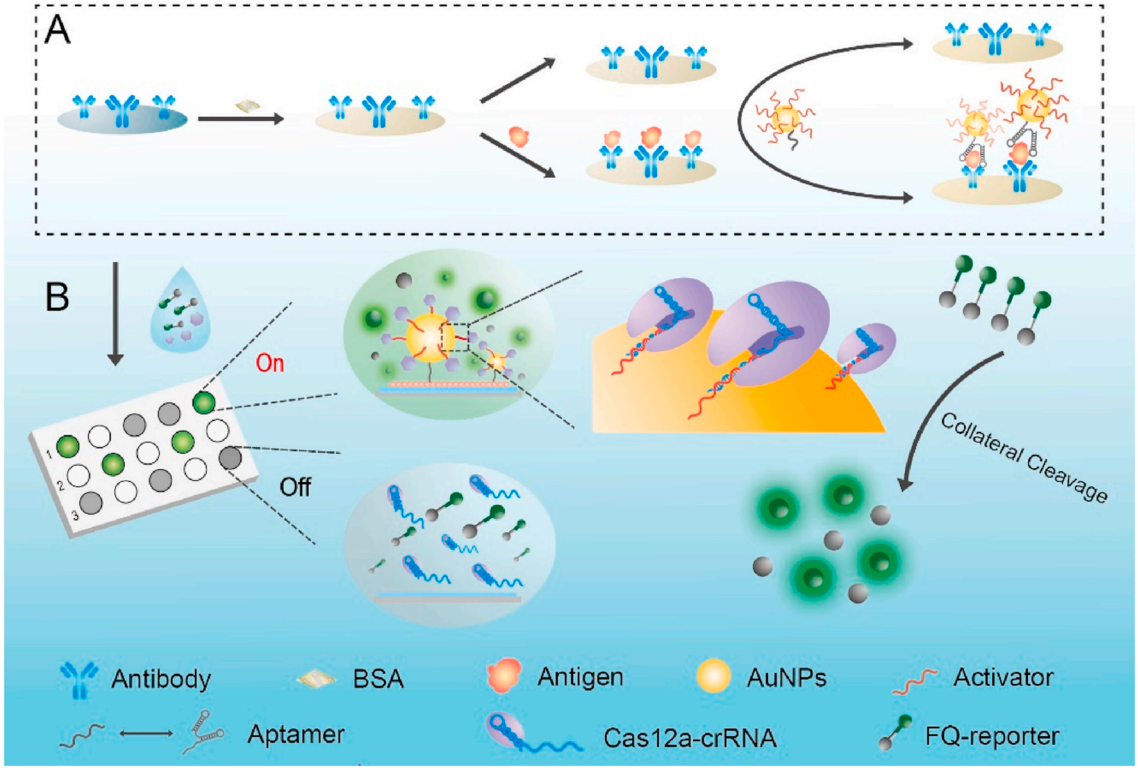

Fig. 1. Schematic illustration of Nano-CLISA for protein detection. (A) Construction of the modified immune sandwich structure. (B) Random cleavage of ssDNA and release of fluorescence signal from FQ-reporters by AuNPs-DNA activated CRISPR/Cas12a.

system.

Proteins act as an important biomarker, whose accurate and quantitative detection is of significance for clinical diagnostics, proteomic research, and other biomedical applications (Engvall and Perlmann, 1971; Uhlén et al., 2019). Enzyme-linked immunosorbent assay (ELISA) (Lai et al., 2004; Yang et al., 2019) is widely regarded as the gold standard for protein biomarker detection due to its high specificity, high throughput, and high applicability. With the increasing demand for an analytical range of analysis and sensitive detection of cancer biomarkers, various technologies have been integrated into ELISA (Cheng et al., 2010; Lee and Zeng, 2017; Yang et al., 2019). Chen et al. (2020) show a new version of ELISA performed via using CRISPR/Cas13a as a signal amplification strategy. Amplification of the target nucleotides by T7 RNA polymerase transcription was essential for signal amplification, which was cost-prohibitive and time-consuming. As an outstanding biological carrier material, gold nanoparticles (AuNPs) were widely applied to biological analysis due to the high loading capacity for different kinds of molecules, such as proteins and nucleic acids (Chen et al., 2014; Liu et al., 2020; Wu et al., 2017; Zhao et al., 2011). To the best of our knowledge, the integration of DNA-AuNPs with CRISPR/Cas system for signal amplification of immunoassay has never been reported.

Here, we designed DNA-modified Au nanoparticles to activate CRISPR/Cas12a for immunosorbent assay (denoted as Nano-CLISA). To construct a universal signal conversion and efficient amplification methodology, AuNPs were covalently modified with aptamer and Cas12a target DNA (activator) simultaneously. With the advantages of low cost, easy synthesis, chemical stability and flexibility (Huang et al., 2019; Kim et al., 2016), aptamers are employed for specific binding protein instead of antibodies in Nano-CLISA. A large number of activators modified on AuNPs can effectively activate the *trans*-cleavage activity of Cas12a, resulting in the breaking of the short ssDNA reporters (FQ-reporter) labeled with fluorophore groups (FAM) and quenchers (BHQ1) at both ends of the sequence. Nano-CLISA shows potential to detect a wide range of biomarkers with high sensitivity. The effectiveness of the method was verified by detecting biomarkers of carcinoembryonic antigen (CEA) and prostate-specific antigen (PSA) at attomolar sensitivity, which was 1000 lower than that of conventional ELISA, and the detection range is 15 times wider than that of conventional ELISA.

2. Experimental section

2.1. Synthesis of oligonucleotide functionalized gold nanoparticles

Oligonucleotides were covalently fixed on the surface of AuNPs through the coordination between thiol modifier group of the DNA and gold (Liu and Lu, 2006). First, the thiol-DNA (aptamers and activators) was activated with 10 mM Tris [2-carboxyethyl] phosphine (TECP) at room temperature for 1 h. AuNPs, aptamers and activators were mixed at a certain molar ratio into the disposable scintillation vials (soak in 12 M NaOH for 1 h before use). After 16 h of shake at room temperature, 1 M NaCl solution was added in batches during shaking to make the final concentration at 0.1 M. The solution was further incubated at room temperature for 24 h. After that, the free DNA was removed by centrifugation, and the precipitation was washed three times with PBS buffer. Finally, the product (13 nM) was dispersed in PBS buffer and stored at 4 °C.

2.2. Procedure of Nano-CLISA reaction

Initially, specific capture antibodies (10 μg/mL) were added to the 96-well polystyrene plate with a dose of 100 μL per well, and incubated overnight at 4 °C. To block the unspecific binding, 200 μL blocking buffer (1% BSA in PBS buffer) was added to each well and incubated for 1 h at 37 °C. 100 μL antigen standard solutions with different concentrations were added to 96-well plate and incubated for 1 h at 37 °C. Subsequently, 100 μL of functionalized AuNPs (1 nM) were added to each well and incubated at 37 °C for 1 h. After each binding incubation,

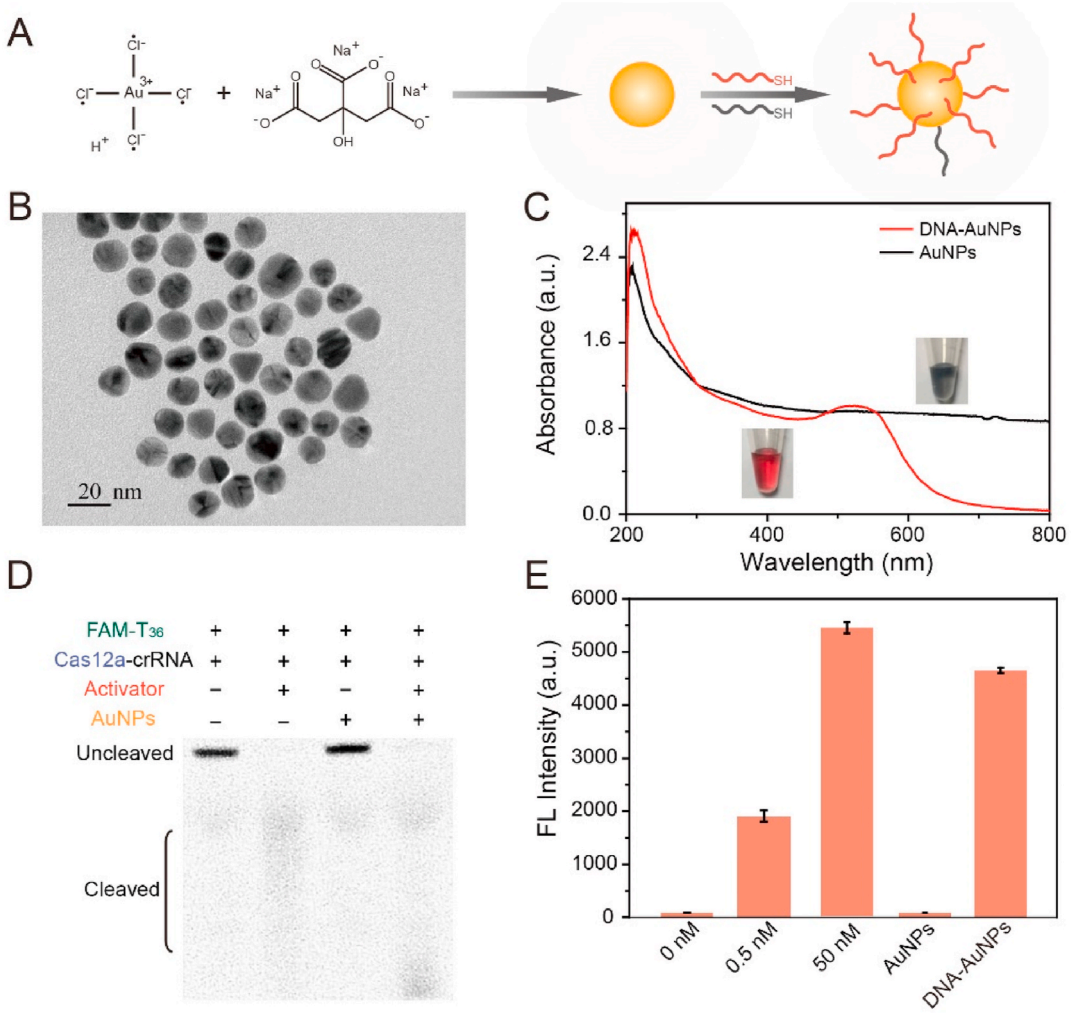

Fig. 2. (A) Schematic illustration of preparation process of AuNP nanoprobes. (B) TEM image of AuNPs. (C) UV–vis absorption spectra of AuNPs before (black) and after (red) modification with DNA in PBS buffer. Inset: pictures showing the color of the corresponding solution. (D) PAGE showing the cleavage of cutting T_{36} with 5′-modified FAM in the absence and presence of the activator. (E) Fluorescence intensity with or without free or covalent activators. Concentrations of activators were 0 nM, 0.5 nM and 50 nM. AuNPs and DNA-AuNPs (AuNPs:Aptamers:Activator = 1:50:100) at the same concentration (0.5 nM). (For interpretation of the references to color in this figure legend, the reader is referred to the Web version of this article.)

the plate was washed at last three times with PBST buffer.

Cas12a was preassembled with crRNA and incubated at room temperature for 10 min. Then, 100 μL CRISPR/Cas12a reaction system (20 nM Cas12a, 250 nM crRNA and 150 nM FQ-reporter in 1 × NEB 2.1 buffer) was added to the wells with different concentrations of antigen. NEB 2.1 buffer was purchased from New England Biolabs Inc. (Ipswich, USA). After incubation at 37 °C for 2 h, the fluorescence signal was measured at room temperature. A fluorescence spectrometer (Hitachi F-4600, Tokyo, Japan) was used for fluorescence measurement (excitation at 480 nm and emission at 520 nm).

2.3. Analysis of clinical serum samples

Serum samples were collected by Nanjing Drum Tower Hospital and frozen at -80 °C immediately. Each serum sample was quantitatively detected by Nano-CLISA and ELISA Kit respectively. The Bland-Altman analysis was realized with MedCalc and the ROC curve was constructed and calculated with SPSS.

3. Results and discussion

3.1. Working principle of the Nano-CLISA

Nano-CLISA detection is a two-step process (Fig. 1): first, an immune-like-sandwich structure was formed where AuNPs were modified with aptamers and activators instead of detection antibodies (Fig. 1A); then, a fluorescence signal amplification process was generated through DNA-AuNPs activating *trans*-cleavage activity of Cas12a (Fig. 1B). In the presence of protein analytes, the sandwich structure of antibody-antigen-AuNP could be formed on the microplate leading to the activation of Cas12a by the activators on the surfaces of AuNPs. Once activated, Cas12a began to cleave nearby FQ-reporters, resulting in segregation of the fluorophore from the quencher and thereby producing a significant enhancement of fluorescence signal. The fluorescence intensity was positively correlated with the concentration of activators, so the level of analytes was indirectly reflected. On the contrary, in the absence of analytes, DNA-AuNPs conjugates were washed away due to the unsuccessful formation of sandwich structure. Thus, the *trans*-cleavage activity of Cas12a could not be triggered and the change of fluorescence signal was nearly negligible. From this, protein can be analyzed quantitatively by reading out the fluorescence signals.

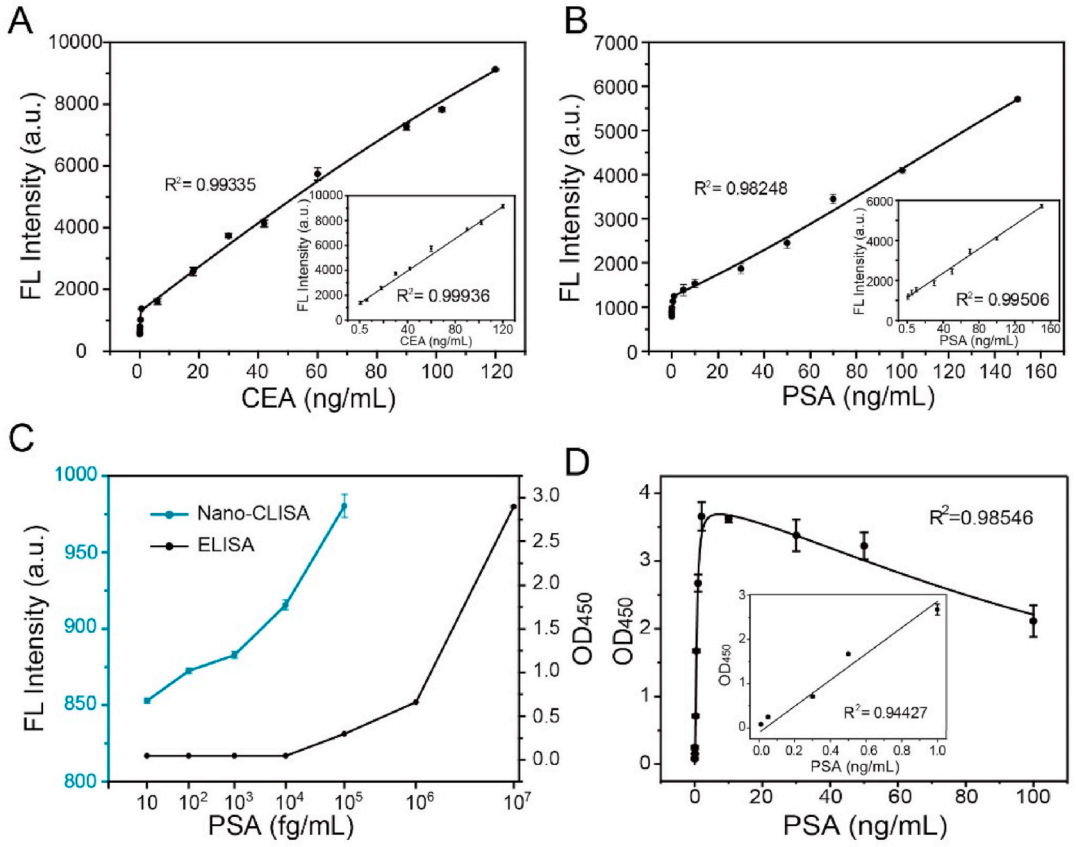

Fig. 3. Quantitative analysis of protein in PBS buffer by the Nano-CLISA method. (A) Relationship between fluorescence intensity and CEA concentration. Inset: linear trend line of CEA in the range of 0.6–120 ng/mL. (B) Relationship between fluorescence intensity and PSA concentration. Inset: linear trend line of PSA in the range of 0.6–120 ng/mL (C) PSA was added to the coated plate at a series of 10-fold dilutions from 10 fg/mL to 100 pg/mL. A calibration curve was established by plotting fluorescence intensity of the concentrations of PSA. A parallel ELISA experiment was also performed at a series of 10-fold dilutions from 10 fg/mL to 10 ng/mL. (D) Optical density at different concentrations of PSA (0–100 ng/mL) in PBS buffer was measured by the ELISA method. The illustration shows the linear trend line of optical density induced by PSA concentrations between 0.1 and 1 ng/mL. Data represent mean ± s.d., n = 3, three technical replicates.

3.2. *Construction of the Nano-CLISA platform*

Serving as essential nanomaterials in Nano-CLISA, DNA functionalized AuNPs were synthesized by the previously reported method as shown in Fig. 2A (Liu and Lu, 2006). Transmission electron microscopy (TEM) characterization (Fig. 2B) and particle size distribution statistics (Fig. S1) show that AuNPs are monodisperse nanospheres with an average particle size of 13 nm. To prove the successful immobilization of oligonucleotides onto the surface of AuNPs, PBS buffer with 0.1 M NaCl was used to test the stability of the DNA functionalized AuNPs in high salt solution. As shown in Fig. 2C, the DNA functionalized AuNPs solution kept in red with a characteristic absorption peak at 520 nm wavelength in ultraviolet–visible (UV–visible) absorption spectrum, while the unmodified AuNPs solution presented blue-gray and the characteristic peak disappeared, which suggests the modified DNA could protect AuNPs from salt-induced aggregation (Storhoff et al., 2002). TEM characterizations further showed that AuNPs without DNA modification formed a large number of aggregates of the AuNPs in high salt solution, while DNA functionalized AuNPs dispersed well (Fig. S2). Furthermore, zeta potential measurements showed that the surface potential of AuNPs decreased after oligonucleotides functionalization (Fig. S3), which could be attributed to the negative charge of oligonucleotides.

As a core of Nano-CLISA platform, the *trans*-cleavage performance of CRISPR/Cas12a in the presence of activator was firstly tested. The cleavage mechanism of CRISPR/Cas12a is shown in Fig. S4A. CRISPR/Cas12a system was incubated with a series of concentrations of free target ssDNA (activator), and then the reaction kinetics was measured (Fig. S4B). The intensities of the fluorescence signals are positively correlated with time, and the cleavage rates rise significantly with the increase of activator concentrations. We also confirmed that the intensity of the fluorescence signal was positively correlated with concentrations of activators (Fig. S4C and S4D). However, the intensity of fluorescence did not continue to increase significantly when the incubation time reached 50 min or the concentration of activators reached 10 nM, which was possibly restricted by concentrations and ratio of CRISPR/Cas12a and FQ-reporters.

Furthermore, we assessed *trans*-cleavage performance of CRISPR/Cas12a activated by ssDNA functionalized AuNPs. As shown in Fig. 2D, the Gel electrophoresis (PAGE) demonstrated that Cas12a exhibited good *trans*-cleavage capability in the presence of activators, whether they were free or covalently coupled to the AuNPs. The fluorescence measurement as depicted in Fig. 2E further proved that the *trans*-cleavage activity of Cas12a could not only be activated by the activator modified AuNPs but also play a role in collaborative signal amplification. Compared with the same concentration of free activators, the fluorescence intensity of the functionalized AuNPs incubated with Cas12a system increased about three times, due to a large number of activators connected to AuNPs. Notably, the fluorescence signal of theoretical amount of DNA modified AuNPs only slightly weakened. Altogether, it concluded that the Nano-CLISA platform is feasible in protein assay.

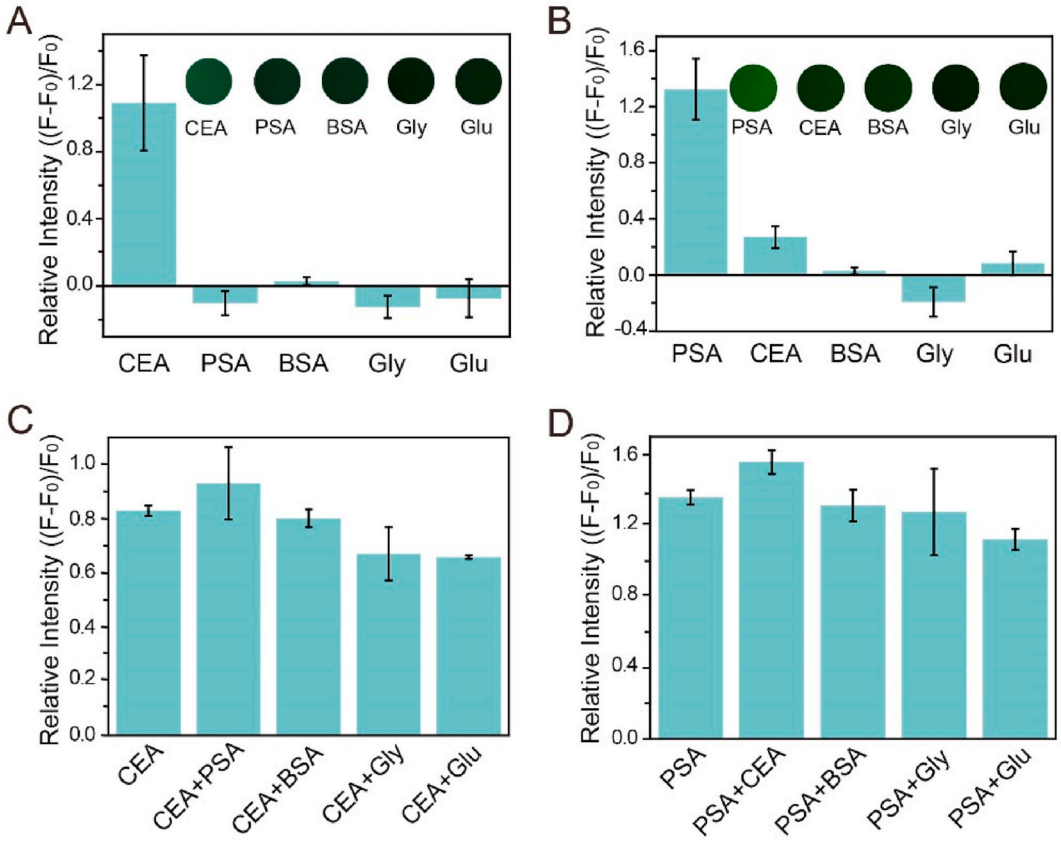

Fig. 4. Study of the specificity of the Nano-CLISA method for the detection of CEA and PSA. (A) Relative fluorescence intensity of the Nano-CLISA system in the presence of CEA (2.5 ng/mL) and other molecules (25 ng/mL) individually. (B) Relative fluorescence intensity of the Nano-CLISA system in the presence of PSA (4 ng/mL) and other molecules (40 ng/mL) individually. (C) Relative fluorescence intensity of the Nano-CLISA system in the presence of CEA (2.5 ng/mL) and other molecules (25 ng/mL) mixed. (D) Relative fluorescence intensity of the Nano-CLISA system in the presence of PSA (4 ng/mL) and other molecules (40 ng/mL) mixed. F_0 and F represent the fluorescence intensity of the Nano-CLISA system at 520 nm in the absence and presence of the protein analyte or other molecules, respectively. (inset: the corresponding fluorescence images; n = 3).

3.3. Optimization of experimental conditions for the Nano-CLISA

To obtain a better signal response and a higher sensitivity, we optimized the experimental conditions. According to previous reports, commercial NEB 2.1 buffer was used as the reaction buffer for Cas12a (Xiong et al., 2020). The performance of functionalized AuNPs was closely related to the proportion of aptamers and activators. On the one hand, too few or too many activators modified on AuNPs were not conducive to amplification of fluorescence signal as shown in Fig. S5A. It was probably because too few activators led to insufficient amplification of fluorescence signal, while a too high density of activators on AuNPs maybe hinder the specific binding of Cas12a to activators in space. On the other hand, as shown in Fig. S5B, too few or too many aptamers modified on AuNPs both led to the drop-in signal. It was probably because too few aptamers would decrease the efficiency of specific antigen recognition, while too many aptamers may compete with activators to couple to AuNPs, resulting in a low concentration of activators on AuNPs. Thus, the molar ratio of 1:50:100 (AuNPs:aptamers:activators) was eventually selected for the preparation of functionalized AuNPs, which provided a compromise between analysis capture and the signal amplification. Based on the Michaelis-Menten equational (Supporting Information), at low substrate (FQ-reporter) concentration, the apparent cleavage rates positively correlated with the FQ-reporter. However, the cleavage rate slows down and tends to be constant when the substrate concentration is high. As shown in Fig. S5C, the FQ-reporter with a final concentration of 200 nM was selected as the experiment condition to ensure the optimal value of fluorescence signal. Under these conditions, the time-dependent fluorescence intensity peaked at 120 min (Fig. S5D). Therefore, these optimized experimental conditions are applied to the following researches.

3.4. Detection of proteins by the Nano-CLISA platform

To determine if the Nano-CLISA platform could detect protein quantitatively, we first detected CEA protein, which is one of the crucial tumor markers responsible for clinical diagnosis of colon, breast, lung, pancreas, ovaries and gastrointestinal tract cancer (Shively and Beatty, 1985). We measured the fluorescence spectra of different concentrations of CEA added in PBS buffer (Fig. S6A). As shown in Fig. 3A, the fluorescence signal at 520 nm increased with CEA concentrations from 0 to 120 ng/mL, and there is a linear trend in the range of 0.6–120 ng/mL. The fluorescence intensity (30 fg/mL of CEA in presence) is higher than the background and the limit of detection (LOD) was calculated to be 13.9 fg/mL (69.5 aM) based on 3-fold the standard deviation of blank signals (n = 3) to the slope of linearity presented in the low concentration group (Fig. S7A).

Since the strategy mainly depends on the specific recognition of aptamer and antibody toward targets, it has the potential to be extended to the detection of a variety of biomarkers. To demonstrate the universality of the platform, PSA, a significant biomarker for prostate cancer early diagnosis and subsequent treatment (Kong et al., 2015), was selected as the target of interest. We measured the fluorescence spectra of different concentrations of PSA added in PBS buffer (Fig. S6B). As shown in Fig. 3B, the fluorescence signal at 520 nm increased with PSA concentrations from 0 to 150 ng/mL, and there is a linear trend in the range of 0.5–150 ng/mL, which was about 15-fold wider than the

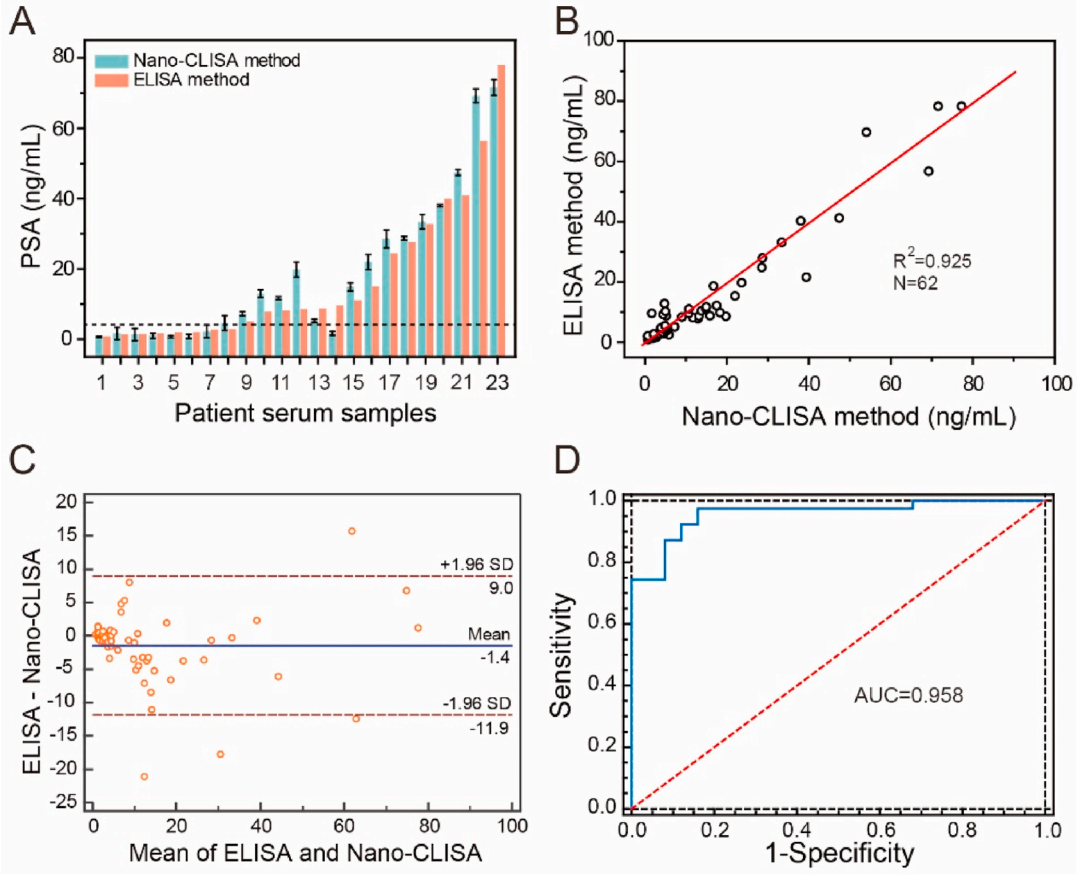

Fig. 5. Analysis of PSA in clinical serum samples. (A) Quantitation of PSA by the Nano-CLISA method compared with standard ELISA for 23 serum samples. Error bars indicated the standard deviations in triplicate experiments. The dashed line represents the clinical cut-off value of 4 ng/mL. (B) Consistency between data obtained from the two methods. Red lines represent y = x, and R^2 was calculated by the function y = x instead of the fitting function. (C) Bland-Altman plots between the Nano-CLISA method and ELISA method for PSA detection. (D) The receiver-operating characteristic (ROC) analysis for PSA assay of serum samples. (For interpretation of the references to color in this figure legend, the reader is referred to the Web version of this article.)

commercial human PSA ELISA kit (0.01 ng/mL) (Fig. 3D). It can be more suitable for the direct detection of high concentrations (>10 ng/mL) without sample dilution procedure like ELISA. The fluorescence intensity (10 fg/mL of PSA in presence) is higher than the background and the LOD was calculated to be 5.6 fg/mL (175 aM) (Fig. S7B), which was about 1000-fold lower than the commercial human PSA ELISA kit (0.01 ng/mL) (Fig. 3C). In addition, we compared Nano-CLISA with several other methods (Table S2). This work shows that the Nano-CLISA method is superior in sensitivity and dynamic detection ranges to most of the reported fluorescence or chemiluminescence detection systems.

Next, four kinds of signal transduction strategies (aptamer, an aptamer strand includes one or two repetitive activator units on a single DNA, DNA-AuNPs) were compared in detection of CEA and PSA (Fig. S8). The results show that the fluorescence signal intensity of DNA-AuNPs as signal transduction strategy was significantly higher than that of others (See supporting information for detailed discussion). In addition to a large number of activators on AuNPs to amplify signals, the Cas12a enzyme also has an approximation (Supporting Information).

3.5. *Verification of specificity of the Nano-CLISA platform*

To evaluate the specificity of the platform-based CRISPR/Cas12a, other biological substances were introduced as interferents. In the study of the selectivity, the concentrations of all interferents were set ten times higher than that of analytes. As can be seen in Fig. 4A and B, the variation of fluorescence signal caused by analytes could be distinctly separate from other biomolecules. Moreover, the measurement of analytes together with interferents also certificated the platform could be used for concurrent test of analytes and other biomolecules without interference between each other (Fig. 4C and D). These results indicated that Nano-CLISA could detect analytes specifically, due to the excellent specific affinity of aptamers and antibodies to analytes without the interference of other biomolecules.

3.6. *Application of the Nano-CLISA platform in clinical sample detection*

The correctness of clinical analysis is one of the key factors to assess the implementation effect of the new strategy. The different human serum samples from sixty-two donors were analyzed for PSA levels by the Nano-CLISA and commercial ELISA Kit respectively. The distinction between positive and negative signals relies on the widely adopted clinical threshold (4 ng/mL) (Gustafsson et al., 1998), which is represented by the horizontal dashed line (Fig. 5A). Due to operation and sample storage, false positives or false negatives often occur in the detection of clinical serum samples, especially near the cut-off value (such as samples 13, 14). We estimated the consistency of the serum test between Nano-CLISA and ELISA. Fig. 5B indicated that the two methods showed excellent consistency. Most of the results were within the range of 1.96 SD in the Bland-Altman assay (Fig. 5C), suggesting that the platform has great consistency with the gold standard method of ELISA. Finally, the receiver operating characteristic (ROC) curve for PSA detection (Fig. 5D) was established. As Fig. 5D described, the area under the curve (AUC) was 0.958 (95% CI: 0.912–1.000, $P < 0.0001$), the best cut-off value was 3.70 ng/mL with a clinical sensitivity of 97.4% and

specificity of 84%. Results indicated that the platform has high precision. Ultimately, these results suggest that the platform is capable of reliably analyzing PSA in clinical samples.

4. Conclusion

In this work, a nano-immunosorbent assay based on Cas12a/crRNA (Nano-CLISA) was developed to ultra-sensitively detect proteins. Activators and aptamers functionalized gold nanoparticles (AuNPs) as a universal signal transduction strategy were employed as both a recognizer and a nano-switch to trigger the *trans*-cleavage activity of Cas12a. The hundreds of thiol-oligonucleotides on AuNPs for activation of CRISPR/Cas12a played a good role in signal enhancement. Using CEA and PSA as model analytes, the LOD could attain as low as 13.9 fg/mL (69.5 aM) and 5.6 fg/mL (175 aM) respectively, exhibiting a 1000-fold improvement compared with commercialized ELISA Kits. This platform was also successfully applied to analyze PSA levels in clinical samples. An automated and high-throughput format is expected to be integrated with Nano-CLISA in the future to develop a rapid screening of large numbers of samples simultaneously that can be easily used. It is worth mentioning that the platform is flexible and promising for the analysis of other molecules beyond protein. We hope that the construction strategy of the CRISPR/Cas12a analysis platform can provide some inspiration for the application of the CRISPR/Cas system in biological diagnosis.

CRediT authorship contribution statement

Qiao Zhao: Conceptualization, Methodology, Validation, Formal analysis, Investigation, Data curation, Writing – original draft. **Yongchun Pan:** Methodology, Writing – review & editing. **Xiaowei Luan:** Writing – review & editing. **Yanfeng Gao:** Writing – review & editing. **Xiaozhi Zhao:** Resources. **Yinghui Liu:** Resources. **Yuzhen Wang:** Conceptualization, Supervision, Project administration, Funding acquisition, Writing – review & editing. **Yujun Song:** Conceptualization, Supervision, Project administration, Funding acquisition, Writing – review & editing.

Declaration of competing interest

The authors declare that they have no known competing financial interests or personal relationships that could have appeared to influence the work reported in this paper.

Acknowledgements

This work was financially supported by the National Key R&D Program of China (2019YFA0709200), the National Natural Science Foundation of China (21874066, 81601632 and 61804076), the Natural Science Foundation of Jiangsu Province (BK20180700 and BK20200336), the Fundamental Research Funds for Central Universities and the Program for Innovative Talents and Entrepreneur in Jiangsu.

Appendix A. Supplementary data

Supplementary data to this article can be found online at https://doi.org/10.1016/j.bios.2021.113450.

References

Ackerman, C.M., Myhrvold, C., Thakku, S.G., Freije, C.A., Metsky, H.C., Yang, D.K., Ye, S. H., Boehm, C.K., Kosoko-Thoroddsen, T.F., Kehe, J., Nguyen, T.G., Carter, A., Kulesa, A., Barnes, J.R., Dugan, V.G., Hung, D.T., Blainey, P.C., Sabeti, P.C., 2020. Massively multiplexed nucleic acid detection with Cas13. Nature 582 (7811), 277–282.

Bao, Y., Jiang, Y., Xiong, E., Tian, T., Zhang, Z., Lv, J., Li, Y., Zhou, X., 2020. CUT-LAMP: contamination-free loop-mediated isothermal amplification based on the CRISPR/Cas9 cleavage. ACS Sens. 5 (4), 1082–1091.

Bikard, D., Barrangou, R., 2017. Using CRISPR-Cas systems as antimicrobials. Curr. Opin. Microbiol. 37, 155–160.

Broughton, J.P., Deng, X., Yu, G., Fasching, C.L., Servellita, V., Singh, J., Miao, X., Streithorst, J.A., Granados, A., Sotomayor-Gonzalez, A., Zorn, K., Gopez, A., Hsu, E., Gu, W., Miller, S., Pan, C.Y., Guevara, H., Wadford, D.A., Chen, J.S., Chiu, C.Y., 2020. CRISPR-Cas12-based detection of SARS-CoV-2. Nat. Biotechnol. 38 (7), 870–874.

Chen, F., Hou, S., Li, Q., Fan, H., Fan, R., Xu, Z., Zhala, G., Mai, X., Chen, X., Chen, X., Liu, Y., 2014. Development of atom transfer radical polymer-modified gold nanoparticle-based enzyme-linked immunosorbent assay (ELISA). Anal. Chem. 86 (20), 10021–10024.

Chen, J.S., Ma, E., Harrington, L.B., Da Costa, M., Tian, X., Palefsky, J.M., Doudna, J.A., 2018. CRISPR-Cas12a target binding unleashes indiscriminate single-stranded DNase activity. Science 360 (6387), 436–439.

Chen, Q., Tian, T., Xiong, E., Wang, P., Zhou, X., 2020. CRISPR/Cas13a signal amplification linked immunosorbent assay for femtomolar protein detection. Anal. Chem. 92 (1), 573–577.

Cheng, C.M., Martinez, A.W., Gong, J., Mace, C.R., Phillips, S.T., Carrilho, E., Mirica, K. A., Whitesides, G.M., 2010. Paper-based ELISA. Angew Chem. Int. Ed. Engl. 49 (28), 4771–4774.

Engvall, E., Perlmann, P., 1971. Enzyme-linked immunosorbent assay (ELISA) quantitative assay of immunoglobulin. G. Immunochemistry 8 (9), 871–874.

Gootenberg, J.S., Abudayyeh, O.O., Kellner, M.J., Joung, J., Collins, J.J., Zhang, F., 2018. Multiplexed and portable nucleic acid detection platform with Cas13, Cas12a, and Csm6. Science 360 (6387), 439–444.

Gootenberg, J.S., Abudayyeh, O.O., Lee, J.W., Essletzbichler, P., Dy, A.J., Joung, J., Verdine, V., Donghia, N., Daringer, N.M., Freije, C.A., Myhrvold, C., Bhattacharyya, R.P., Livny, J., Regev, A., Koonin, E.V., Hung, D.T., Sabeti, P.C., Collins, J.J., Zhang, F., 2017. Nucleic acid detection with CRISPR-Cas13a/C2c2. Science 356 (6336), 438–442.

Gustafsson, O., Mansour, E., Norming, U., Carlsson, A., Törnblom, M., Nyman, C., 1998. Prostate-specific antigen (PSA), PSA density and age-adjusted PSA reference values in screening for prostate cancer: a study of a randomly selected population of 2,400 men. Scand. J. Urol. Nephrol. 32 (6), 373–377.

He, Q., Yu, D., Bao, M., Korensky, G., Chen, J., Shin, M., Kim, J., Park, M., Qin, P., Du, K., 2020. High-throughput and all-solution phase African Swine Fever Virus (ASFV) detection using CRISPR-Cas12a and fluorescence based point-of-care system. Biosens. Bioelectron. 154, 112068.

Huang, T., Yang, J., Zhou, W., Liu, X., Pan, Y., Song, Y., 2019. Rapid identification of urinary tract infections based on ultrasensitive bacteria detection using volumetric bar-chart chip. Sensor. Actuator. B Chem. 298, 126885.

Jinek, M., Chylinski, K., Fonfara, I., Hauer, M., Doudna, J.A., Charpentier, E., 2012. A programmable dual-RNA–guided DNA endonuclease in adaptive bacterial immunity. Science 337 (6096), 816–821.

Kim, Y.S., Raston, N.H., Gu, M.B., 2016. Aptamer-based nanobiosensors. Biosens. Bioelectron. 76, 2–19.

Kong, R.-M., Ding, L., Wang, Z., You, J., Qu, F., 2015. A novel aptamer-functionalized MoS2 nanosheet fluorescent biosensor for sensitive detection of prostate specific antigen. Anal. Bioanal. Chem. 407 (2), 369–377.

Lai, S., Wang, S., Luo, J., Lee, L.J., Yang, S.-T., Madou, M.J., 2004. Design of a compact disk-like microfluidic platform for enzyme-linked immunosorbent assay. Anal. Chem. 76 (7), 1832–1837.

Lee, K.H., Zeng, H., 2017. Aptamer-based ELISA assay for highly specific and sensitive detection of zika NS1 protein. Anal. Chem. 89 (23), 12743–12748.

Li, H., Xing, S., Xu, J., He, Y., Lai, Y., Wang, Y., Zhang, G., Guo, S., Deng, M., Zeng, M., Liu, W., 2021. Aptamer-based CRISPR/Cas12a assay for the ultrasensitive detection of extracellular vesicle proteins. Talanta 221, 121670.

Li, J., Yang, S., Zuo, C., Dai, L., Guo, Y., Xie, G., 2020. Applying CRISPR-cas12a as a signal amplifier to construct biosensors for non-DNA targets in ultralow concentrations. ACS Sens. 5 (4), 970–977.

Li, S.Y., Cheng, Q.X., Liu, J.K., Nie, X.Q., Zhao, G.P., Wang, J., 2018. CRISPR-Cas12a has both cis- and trans-cleavage activities on single-stranded DNA. Cell Res. 28 (4), 491–493.

Liang, M., Li, Z., Wang, W., Liu, J., Liu, L., Zhu, G., Karthik, L., Wang, M., Wang, K.F., Wang, Z., Yu, J., Shuai, Y., Yu, J., Zhang, L., Yang, Z., Li, C., Zhang, Q., Shi, T., Zhou, L., Xie, F., Dai, H., Liu, X., Zhang, J., Liu, G., Zhuo, Y., Zhang, B., Liu, C., Li, S., Xia, X., Tong, Y., Liu, Y., Alterovitz, G., Tan, G.Y., Zhang, L.X., 2019. A CRISPR-Cas12a-derived biosensing platform for the highly sensitive detection of diverse small molecules. Nat. Commun. 10 (1), 3672.

Lin, W., Tian, T., Jiang, Y., Xiong, E., Zhu, D., Zhou, X., 2021. A CRISPR/Cas9 eraser strategy for contamination-free PCR end-point detection. Biotechnol. Bioeng. 118 (5), 2053–2066.

Liu, J., Lu, Y., 2006. Preparation of aptamer-linked gold nanoparticle purple aggregates for colorimetric sensing of analytes. Nat. Protoc. 1 (1), 246–252.

Liu, X., Pan, Y., Yang, J., Gao, Y., Huang, T., Luan, X., Wang, Y., Song, Y., 2020. Gold nanoparticles doped metal-organic frameworks as near-infrared light-enhanced cascade nanozyme against hypoxic tumors. Nano Research 13 (3), 653–660.

Nam, J.-M., Thaxton, C.S., Mirkin, C.A., 2003. Nanoparticle-based bio-bar codes for the ultrasensitive detection of proteins. Science 301 (5641), 1884–1886.

Pan, Y., Yang, J., Luan, X., Liu, X., Li, X., Yang, J., Huang, T., Sun, L., Wang, Y., Lin, Y., Song, Y., 2019. Near-infrared upconversion–activated CRISPR-Cas9 system: a remote-controlled gene editing platform. Science Advances 5 (4), eaav7199.

Qian, C., Wang, R., Wu, H., Zhang, F., Wu, J., Wang, L., 2019. Uracil-mediated new photospacer-adjacent motif of Cas12a to realize visualized DNA detection at the single-copy level free from contamination. Anal. Chem. 91 (17), 11362–11366.

Shively, J.E., Beatty, J.D., 1985. Cea-related antigens: molecular biology and clinical significance. Crit. Rev. Oncol. Hematol. 2 (4), 355–399.
Storhoff, J.J., Elghanian, R., Mirkin, C.A., Letsinger, R.L., 2002. Sequence-dependent stability of DNA-modified gold nanoparticles. Langmuir 18 (17), 6666–6670.
Strecker, J., Jones, S., Koopal, B., Schmid-Burgk, J., Zetsche, B., Gao, L., Makarova, K.S., Koonin, E.V., Zhang, F., 2019. Engineering of CRISPR-Cas12b for human genome editing. Nat. Commun. 10 (1), 212.
Uhlén, M., Karlsson, M.J., Hober, A., Svensson, A.S., Scheffel, J., Kotol, D., Zhong, W., Tebani, A., Strandberg, L., Edfors, F., Sjöstedt, E., Mulder, J., Mardinoglu, A., Berling, A., Ekblad, S., Dannemeyer, M., Kanje, S., Rockberg, J., Lundqvist, M., Malm, M., Volk, A.L., Nilsson, P., Månberg, A., Dodig-Crnkovic, T., Pin, E., Zwahlen, M., Oksvold, P., von Feilitzen, K., Häussler, R.S., Hong, M.G., Lindskog, C., Ponten, F., Katona, B., Vuu, J., Lindstrom, E., Nielsen, J., Robinson, J., Ayoglu, B., Mahdessian, D., Sullivan, D., Thul, P., Danielsson, F., Stadler, C., Lundberg, E., Bergström, G., Gummesson, A., Voldborg, B.G., Tegel, H., Hober, S., Forsström, B., Schwenk, J.M., Fagerberg, L., Sivertsson, A., 2019. The human secretome. Sci. Signal. 12 (609), eaaz0274.
van Dongen, J.E., Berendsen, J.T.W., Steenbergen, R.D.M., Wolthuis, R.M.F., Eijkel, J.C. T., Segerink, L.I., 2020. Point-of-care CRISPR/Cas nucleic acid detection: recent advances, challenges and opportunities. Biosens. Bioelectron. 166, 112445.
Wu, Y., Guo, W., Peng, W., Zhao, Q., Piao, J., Zhang, B., Wu, X., Wang, H., Gong, X., Chang, J., 2017. Enhanced fluorescence ELISA based on HAT triggering fluorescence "Turn-on" with enzyme-antibody dual labeled AuNP probes for ultrasensitive detection of AFP and HBsAg. ACS Appl. Mater. Interfaces 9 (11), 9369–9377.
Xiong, Y., Zhang, J., Yang, Z., Mou, Q., Ma, Y., Xiong, Y., Lu, Y., 2020. Functional DNA regulated CRISPR-cas12a sensors for point-of-care diagnostics of non-nucleic-acid targets. J. Am. Chem. Soc. 142 (1), 207–213.
Yang, J., Liu, X., Pan, Y., Yang, J., He, B., Fu, Y., Song, Y., 2019. A self-powered microfluidic chip integrated with fluorescent microscopic counting for biomarkers assay. Sensor. Actuator. B Chem. 291, 192–199.
Yin, K., Ding, X., Li, Z., Zhao, H., Cooper, K., Liu, C., 2020. Dynamic aqueous multiphase reaction system for one-pot CRISPR-cas12a-based ultrasensitive and quantitative molecular diagnosis. Anal. Chem. 92 (12), 8561–8568.
Zetsche, B., Gootenberg, J.S., Abudayyeh, O.O., Slaymaker, I.M., Makarova, K.S., Essletzbichler, P., Volz, S.E., Joung, J., van der Oost, J., Regev, A., Koonin, E.V., Zhang, F., 2015. Cpf1 is a single RNA-guided endonuclease of a class 2 CRISPR-Cas system. Cell 163 (3), 759–771.
Zhao, J., Zhang, Y., Li, H., Wen, Y., Fan, X., Lin, F., Tan, L., Yao, S., 2011. Ultrasensitive electrochemical aptasensor for thrombin based on the amplification of aptamer-AuNPs-HRP conjugates. Biosens. Bioelectron. 26 (5), 2297–2303.
Zhao, X., Zeng, L., Mei, Q., Luo, Y., 2020. Allosteric probe-initiated wash-free method for sensitive extracellular vesicle detection through dual cycle-assisted CRISPR-cas12a. ACS Sens. 5 (7), 2239–2246.